Double-Dot Quantum Ratchet Driven by an Independently Biased Quantum Point Contact

V. S. Khrapai,[1,2] S. Ludwig,[1] J. P. Kotthaus,[1] H. P. Tranitz,[3] and W. Wegscheider[3]

[1]*Center for NanoScience and Department für Physik, Ludwig-Maximilians-Universität,*
Geschwister-Scholl-Platz 1, D-80539 München, Germany

[2]*Institute of Solid State Physics RAS, Chernogolovka, 142432, Russian Federation*

[3]*Institut für Experimentelle und Angewandte Physik, Universität Regensburg, D-93040 Regensburg, Germany*

We study a double quantum dot (DQD) coupled to a strongly biased quantum point contact (QPC), each embedded in independent electric circuits. For weak interdot tunneling we observe a finite current flowing through the Coulomb blockaded DQD in response to a strong bias on the QPC. The direction of the current through the DQD is determined by the relative detuning of the energy levels of the two quantum dots. The results are interpreted in terms of a quantum ratchet phenomenon in a DQD energized by a nearby QPC.

In the absence of spatial symmetry, directed particle flow is possible in a system subjected to fluctuations, without any externally applied bias. The second law of thermodynamics requires the fluctuations to be in nonequilibrium [1]; i.e., a directed flow only occurs in response to external energy supply. Systems possessing current because of broken spatial symmetry, so-called ratchets, appear in a variety of examples from biological systems to SQUIDs [2].

In mesoscopic semiconductors, ratchet-type systems have been realized on the basis of a two-dimensional electron gas in GaAs/AlGaAs heterostructures [3]. Spatial asymmetry results in rectified current in periodic ratchets [3], single quantum dots [4], and ballistic rectifiers [5]. Competition of classical motion and quantum tunneling can cause a crossover from a classical to a quantum ratchet as the temperature is decreased [3,6].

A double quantum dot (DQD) with internally broken symmetry, with respect to its charge distribution, can operate as a quantum ratchet. For weak interdot tunneling, detuning of the quantum dots' energy levels results in localization of an electron in one dot, so that the elastic tunneling to the other dot is energetically forbidden. Externally supplied energy quanta can promote inelastic interdot tunneling, leading to a net current flow through the DQD, as observed, e.g., in photon-assisted tunneling (PAT) experiments [7].

In this work a novel dynamic interaction effect between a DQD and an independently biased quantum point contact (QPC) is reported. We observe a finite current through the DQD in response to a strong bias on the QPC. The results are interpreted in terms of a quantum ratchet phenomenon.

Our samples are prepared on a GaAs/AlGaAs heterostructure containing a two-dimensional electron gas 90 nm below the surface, with electron density $n_S = 2.8 \times 10^{11}$ cm^{-2} and mobility $\mu = 1.4 \times 10^6$ cm^2/V s at a temperature of 1.5 K. The AFM micrograph of the split-gate nanostructure, produced with *e*-beam lithography, is shown in Fig. 1(a). The negatively biased central gate *C* is used to divide the electron system into two parts, so that

direct leakage current between them is absent. The DQD is defined and controlled by negative voltages applied to the gates 1–5. Both serially coupled quantum dots possess single-particle level spacings on the order of 100 μeV and charging energies of about 1.5 meV. The DQD has small tunnel couplings of $\Gamma \approx 40$ μeV to the leads and a much smaller interdot tunnel coupling of $t_0 \sim 0.1$ μeV. The QPC is formed on the opposite side of gate *C* by use of gate 8 as well as side gates 7 and 9. The one-dimensional (1D) subband spacing of the QPC is $\Delta E_S \approx 4$ meV and the
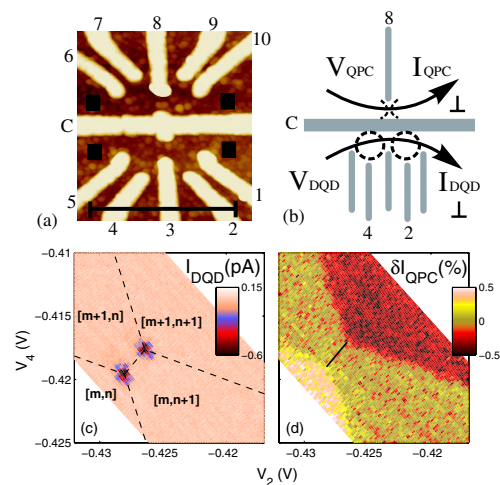

FIG. 1 (color online). (a) AFM micrograph of the sample. Metal surface gates have a light color. Black squares mark source and drain regions. The black scale bar marks a length of 1 μm. (b) Schematic layout of the device as used for all presented measurements. (c) DQD stability diagram for $V_{DQD} = -20$ μV and an unbiased QPC. The axes show gate voltages on the plunger gates 2 and 4. (d) Same area of the stability diagram as in (c) detected with the QPC for $V_{QPC} = -1.45$ mV. A linear trend is subtracted from the I_{QPC} data. In (c) and (d) the QPC gate voltages are $V_8 = -0.597$ V and $V_7 = V_9 = -0.55$ V. $V_6 = V_{10} = 0$ throughout the Letter. The black lines in (c) and (d) are guides to the eyes (see text).

energy window for opening a 1D subband is approximately
1 meV wide [8].

A schematic layout of the device is shown in Fig. 1(b).
Separated circuiting allows both, independent biasing and
a simultaneous current measurement of the DQD and the
QPC. In each circuit the source bias is applied to the left
lead while the right leads are grounded, so that positive
(negative) current corresponds to electrons moving from
the right to the left (or vice versa). We checked that the
results are independent of the particular grounding con-
figuration. The experiments are performed in a dilution
refrigerator at an electron temperature below 150 mK. A dc
current is measured using low noise current-voltage am-
plifiers. Differential conductance data are obtained by
numerical derivation of the dc signal.

First, we discuss a conductance measurement of the
DQD and demonstrate the operation of the QPC as a charge
sensor [9]. Figure 1(c) shows a color scale plot of current
I_{DQD} flowing through the DQD in dependence of voltages
on gates 2 and 4. Here, a small source-drain bias of $V_{DQD} =$
-20 μV is applied to the DQD, while the QPC is kept
unbiased. Gate voltages V_2 and V_4 predominantly control
the occupation of electronic states in the right and left dots,
respectively, allowing to scan a two-dimensional stability
diagram of the DQD [7]. As expected for weak interdot
tunneling, I_{DQD} is nonzero only in the vicinity of the so-
called triple points, where Coulomb blockade is lifted and
electronlike or holelike resonant tunneling occurs [7].
Dashed guide lines in Fig. 1(c) mark the boundaries be-
tween the regions of different ground state charge configu-
rations of the DQD. The charge configuration of the DQD
is denoted as $[m, n]$, corresponding to m (n) electrons
occupying the left (right) dot.

In Fig. 1(d) we plot the current I_{QPC} flowing through the
biased QPC for the same part of the DQD stability diagram
as shown in (c). I_{QPC} increases stepwise each time one
electron leaves the DQD, as a result of electrostatic inter-
action between the electrons traversing the QPC and those
localized in the DQD [9]. Because of the symmetric device
geometry [Fig. 1(a)], no change of I_{QPC} is observed when
repositioning of an electron between the two quantum dots
occurs [across the solid line in Fig. 1(d)] [10].

In the following we report on a new dynamic effect of a
QPC-driven current through a DQD. We bias the QPC at
$V_{QPC} = -1.45$ mV while leaving the DQD at the small
bias of $V_{DQD} = -20$ μV [11]. The dc conductance of the
QPC is adjusted to approximately 0.5 G_0, where $G_0 =$
$2e^2/h$ is the conductance quantum. Figure 2(a) shows the
raw data of I_{DQD} for the same part of the stability diagram
as characterized before [Fig. 1(c)]. Remarkably, away from
the triple points, in the regime of the ground state Coulomb
blockade, we observe a finite current through the DQD,
driven by the QPC bias [compare Figs. 1(c) and 2(a)].
Figure 2(b) shows I_{DQD} for the effectively unbiased DQD
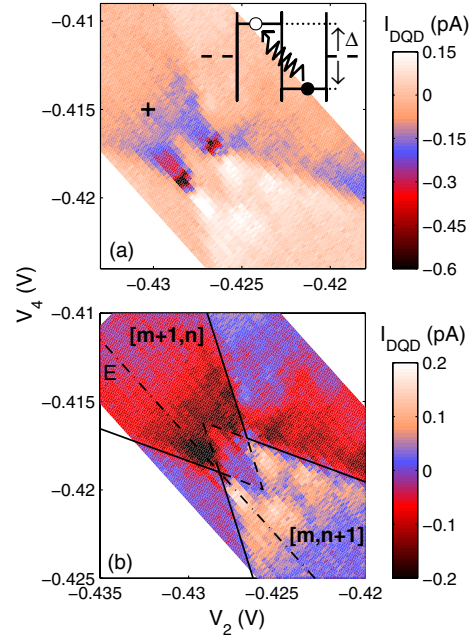[11], obtained after subtraction of the contribution of reso-

FIG. 2 (color online). Current through the DQD while the QPC
is biased with $V_{QPC} = -1.45$ mV. The stability diagram area
and gate voltages are the same as in Fig. 1. (a) Raw data
measured at $V_{DQD} = -20$ μV. (b) The same data after subtrac-
tion of the resonant tunneling contribution at the triple points
(see text). The solid lines in (b) mark boundaries between
regions of stable charge configurations. Dashed and dashed-
dotted lines are explained in the main text. Inset: a sketch of
an inelastic interdot tunneling process involving absorption of an
energy quantum. Horizontal dashed lines mark the leads chemi-
cal potential. The ground and excited electron states are marked
by a filled vs an empty circle, respectively.

nant tunneling at the triple points from the raw data
[Fig. 2(a)]. The DQD signal changes abruptly at the
boundaries of the stability diagram [solid lines in
Fig. 2(b)] and at the edges of a diamond-shaped region
between the triple points (surrounded by dashed lines
continuing the solid lines). Within this diamond I_{DQD} is
close to zero. Otherwise I_{DQD} changes smoothly within
each area of a fixed ground state configuration. The direc-
tion of I_{DQD} is determined by the DQD charge configura-
tion. Note that the current driven through the DQD is much
smaller than the QPC driving current (e.g., $I_{DQD} \sim$
0.5 pA $\ll I_{QPC} \sim 50$ nA for the data presented in Fig. 2).
These features are not specific to the triple points shown
here, but periodically repeated throughout a broad region
of the stability diagram.

The observed dependence of the current driven through
the DQD on its ground state configuration can be under-
stood in terms of inelastic tunneling, similar to PAT [7]. For
the case of the ground state configuration $[m, n + 1]$, this
process is schematically shown in the inset to Fig. 2(a).
Initially localized in the right dot, the highest energy
electron can resonantly absorb an energy quantum and

tunnel to the left dot (transition $[m, n + 1] \rightarrow [m + 1, n]$ in the DQD configuration). The energy difference between the two charge configurations is called the DQD asymmetry energy $\Delta \equiv E_{m+1,n} - E_{m,n+1}$. The resonance condition requires that the energy quantum is equal to the absolute value of the asymmetry energy $|\Delta|$. In our device, the DQD relaxes back to the ground state mainly via the dot-lead tunneling of electrons, because $\Gamma \gg t_0$. The excited electron escapes to the left lead, whereas another electron enters the right dot from the right lead, resulting in the observed net current through the DQD. Note that compared to the process described above, more probable are inelastic processes involving ionization of one quantum dot towards its adjacent lead [12], followed by recharging from the same lead. These charge fluctuations, however, do not result in a net current.

The relevance of the described current transfer mechanism is confirmed by another observation. Within the diamond-shaped region bounded by dashed lines in Fig. 2(b), both involved DQD configurations, $[m, n + 1]$ and $[m + 1, n]$, are Coulomb blockaded [7]. This results in a suppression of the inelastic DQD current, as observed experimentally (Fig. 2).

Inelastic tunneling processes in a DQD can be used to probe excitation spectrum [13,14]. In Fig. 3 the inelastic contribution to the DQD current I_{DQD} is plotted for two negative values of V_{QPC} as a function of Δ [along line E in Fig. 2(b), where gate voltages have been converted to asymmetry energy [7]]. For clarity, the resonant tunneling peak at $\Delta = 0$, measured at $V_{QPC} = 0$, has been subtracted from the data (see the raw data in the inset of Fig. 3). The lower bias data (solid line) are multiplied by a factor of 3.3. In this way, the two curves scale onto a single one, suggesting identical Δ dependencies. $I_{DQD}(\Delta)$ is a nearly antisymmetric function. The transition between negative and
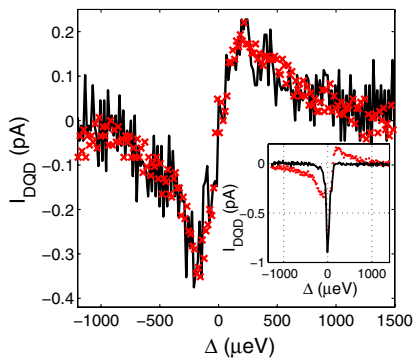
positive current at $\Delta = 0$ has a width of about 150 μeV, much broader than the level width Γ. Hence, the shape of $I_{DQD}(\Delta)$ at small Δ might be related to the low energy falloff in the excitation spectrum. For $|\Delta| \gtrsim 1$ meV I_{DQD} vanishes, suggesting a 250 GHz bandwidth of the excitation spectrum. Note that the charging energy, which limits the bandwidth of a DQD-based detector, is considerably larger. The broadband spectrum of the DQD excitation results in a sharp contrast between the data in Figs. 2 and 3 and conventional PAT experiments [7,10].

A finite QPC-driven current through the DQD is only detected when the highest energy electron is localized in one of the dots ($\Delta \neq 0$). Thus, an internal asymmetry of the DQD is needed to cause a dc current resulting from single electron tunneling processes between quantized energy levels. This demonstrates that the DQD is a quantum ratchet. The QPC acts as a nonequilibrium energy source driving the DQD quantum ratchet.

In the following we study the ratchet driving mechanism by changing the transmission and source bias of the QPC, while the DQD ratchet is adjusted to a fixed asymmetry energy $\Delta = -450$ μeV [as marked by a black cross in Fig. 2(a)]. Figure 4(a) shows the measured current I_{DQD} as a function of the gate voltage V_8, controlling the transmission of the QPC at a fixed source bias of $V_{QPC} = 1.95$ mV. Also shown are the conductance ($G = I/V$) and the differential conductance ($g = dI/dV$) of the QPC. The plateaus at $G = G_0$ and $G = 2 G_0$ correspond to the onset of full transmission in the first two 1D subbands [8]. The regions of partial transmission between the plateaus are broadened because of the applied bias V_{QPC}. Within these regions the differential conductance shows so-called half plateaus at $g \approx 0.4 G_0$ and $g \approx 1.6 G_0$ [8,15]. The ratchet current I_{DQD} has two local maxima at voltages corresponding to the half plateaus in g. The first maximum above the
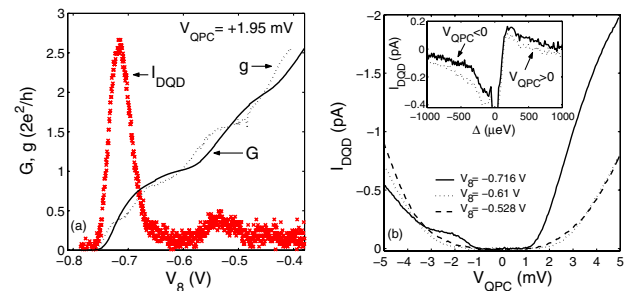

FIG. 3 (color online). Inelastic current I_{DQD} for $V_{QPC} = -1.55$ mV (symbols) and $3.3 \times I_{DQD}$ for $V_{QPC} = -1.15$ mV (solid line), after subtraction of the elastic contribution $I_{DQD}(V_{QPC} = 0)$, as a function of Δ. The data are measured along line E in Fig. 2(b). Gate voltages defining the QPC are the same as for Fig. 1. Inset: raw data measured at $V_{QPC} = 0$ (line) and -1.45 mV (symbols), and $V_{DQD} = -20$ μV.

FIG. 4 (color online). (a) I_{DQD} (a.u.), dc conductance (G), and differential conductance (g) of the QPC for $V_{QPC} = 1.95$ mV as a function of the QPC gate voltage V_8 ($V_7 = V_9 = 0$). (b) I_{DQD} as a function of V_{QPC} for 3 values of V_8, corresponding to the two local maxima of I_{DQD} in (a) and the minimum in between. In both (a) and (b) $\Delta = -450$ μeV. The according position in the stability diagram is marked in Fig. 2(a) by a black cross. Inset: I_{DQD} measured along line E in Fig. 2(b) for $V_{QPC} = \pm 1.45$ mV. All current data shown in Fig. 4 are raw data.

onset of the QPC conduction is much more pronounced than the second one. I_{DQD} is minimal in case of fully transmitting 1D subbands of the QPC. This nonmonotonous dependence of I_{DQD} on the QPC transmission excludes the energy dissipation of electrons in the leads of the QPC as the ratchet driving mechanism. We conclude that the energy source is determined by local dissipation in the QPC.

Figure 4(b) shows I_{DQD} as a function of V_{QPC} for QPC gate voltages tuned to the positions of the two current maxima in Fig. 4(a) or the minimum in between. As expected for a ratchet, I_{DQD} is negative, regardless of the sign of V_{QPC}. Strikingly, at small bias $|V_{QPC}| \lesssim 1$ mV the current through the DQD vanishes. This onset value is independent of Δ (refer to the scaling behavior observed in Fig. 3). As V_{QPC} increases the two maxima broaden, and for $|V_{QPC}| \gtrsim \Delta E_S$ the minimum in between disappears, explaining the dotted curve in Fig. 4(b).

We now discuss a possible ratchet driving mechanism, resulting from the strongly biased QPC. The condition of partial transmission in 1D subbands of the QPC, necessary for $I_{DQD} \neq 0$ [Fig. 4(a)], signals the importance of shot noise [16]. Voltage fluctuations originating from current shot noise is a known excitation mechanism in on-chip detection schemes [12,14]. However, for the DQD ratchet, in this case the onset QPC bias is expected to depend on the DQD asymmetry energy as $V_{QPC} = \Delta/e$, in contrast to our experimental results [17]. We believe that the energy relaxation of electrons traversing the QPC is involved. Occupation number fluctuations, caused by shot noise, lift the Fermi degeneracy of the current carrying 1D electron states. At high bias, unoccupied current carrying states exist within an energy window of about 1 meV near the 1D subband bottom in our QPC. This is expected to enhance the energy relaxation rate of electrons within the QPC. Qualitatively, this could account for the observed nonmonotonic dependence of the ratchet current upon the QPC transmission [Fig. 4(a)]. However, quantitatively, the relative height of the two current maxima [Fig. 4(a)], as well as the suppression of I_{DQD} at $|V_{QPC}| \lesssim 1$ mV [Fig. 4(b)], is lacking explanation. The energy quanta, emitted by the QPC electrons and absorbed by the electrons in the DQD, could be short wavelength acoustic phonons, long wavelength photons, or 1D plasmons. A further discrimination is difficult, because close to the 1D subband bottom no strict constraints are imposed by the momentum conservation law [18].

Finally, we mention an additional contribution to the DQD current, which is not related to the ratchet phenomenon. The inset of Fig. 4(b) plots the measured I_{DQD} as a function of Δ for positive versus negative $V_{QPC} = \pm 1.45$ mV. Clearly, apart from the ratchet current contribution (antisymmetric in Δ), an additional negative and Δ-independent contribution to I_{DQD} is seen for $V_{QPC} > 0$. This contribution to I_{DQD}, which is always opposite to the current in the QPC, is responsible for the bias asymmetry

of one curve seen in Fig. 4(b) (solid line). It can be attributed to a drag-type effect, operating independently of the ratchet phenomenon near the QPC pinch-off, as, e.g., phonon-mediated adiabatic pumping [19] or statistically asymmetric voltage noise [20].

In summary, we find a current through a DQD, driven by a strongly biased nearby QPC. We demonstrate that the DQD acts as a quantum ratchet, energized by the current through the independently biased QPC. The experimental results are qualitatively consistent with inelastic relaxation of electrons in partly transmitting 1D channels of the QPC.

[1] R. P. Feynman, R. B. Leighton, and M. Sands, *The Feynman Lectures on Physics* (Addison-Wesley, Reading, MA, 1963), Vol. 1, Chap. 46.
[2] P. Reimann, Phys. Rep. **361**, 57 (2002); P. Reimann and P. Hänggi, Appl. Phys. A: Mater. Sci. Process. **75**, 169 (2002); S. Kohler, J. Lehmann, and P. Hänggi, Phys. Rep. **406**, 379 (2005).
[3] H. Linke *et al.*, Science **286**, 2314 (1999).
[4] H. Linke *et al.*, Phys. Rev. B **61**, 15 914 (2000).
[5] A. M. Song *et al.*, Phys. Rev. Lett. **80**, 3831 (1998).
[6] P. Reimann, M. Grifoni, and P Hänggi, Phys. Rev. Lett. **79**, 10 (1997).
[7] W. G. van der Wiel, S. De Franceschi, J. M. Elzerman *et al.*, Rev. Mod. Phys. **75**, 1 (2003).
[8] L. I. Glazman and A. V. Khaetskii, JETP Lett. **48**, 591 (1988).
[9] M. Field *et al.*, Phys. Rev. Lett. **70**, 1311 (1993).
[10] J. R. Petta *et al.*, Phys. Rev. Lett. **93**, 186802 (2004).
[11] Direct measurements at $V_{DQD} = 0$ are superimposed by a signal caused by rectification of 50 Hz noise ($\simeq 10$ μV rms). This we avoid by using a finite bias of $V_{DQD} = -20$ μV. We find the QPC-driven current through the DQD to be independent of bias for $|V_{DQD}| < 50$ μV.
[12] E. Onac *et al.*, Phys. Rev. Lett. **96**, 176601 (2006).
[13] T. Fujisawa *et al.*, Science **282**, 932 (1998).
[14] R. Aguado and L. P. Kouwenhoven, Phys. Rev. Lett. **84**, 1986 (2000).
[15] A. Kristensen *et al.*, Phys. Rev. B **62**, 10 950 (2000).
[16] Ya. M. Blanter and M. Buettiker, Phys. Rep. **336**, 1 (2000).
[17] For the parameters of our system, we estimate [14] that the current I_{DQD}, caused by the shot noise voltage fluctuations on the QPC, is at least 3 orders of magnitude smaller than the experimentally found ratchet current.
[18] G. Seelig and K. A. Matveev, Phys. Rev. Lett. **90**, 176804 (2003).
[19] Y. Levinson, O. Entin-Wohlman, and P. Woelfle, Phys. Rev. Lett. **85**, 634 (2000).
[20] J. Luczka, R Bartussek, and P. Hänggi, Europhys. Lett. **31**, 431 (1995); P. Hänggi *et al.*, Europhys. Lett. **35**, 315 (1996).